Solubilisation of salicylate in F127 micelles: effect of pH and temperature on morphology and interactions with cyclodextrin

Margarita Valero,*[a] Wenjing Hu[b], Judith E. Houston[c,d], Cécile A. Dreiss[b]

[a] Dpto. Química Física, Facultad de Farmacia, Universidad de Salamanca, Campus Miguel de Unamuno, s/n, 37007 Salamanca, Spain

[b] Institute of Pharmaceutical Science, King's College London, Franklin-Wilkins Building, 150 Stamford Street, London SE1 9NH, U.K.

[c] Jülich Centre for Neutron Science (JCNS) at Heinz Maier-Leibnitz Zentrum (MLZ) Forschungszentrum Jülich GmbH, Lichtenbergstraße 1, 85747 Garching, Germany.

[d] European Spallation Source (ESS), Odarslövsvägen 113, 225 92 Lund, Sweden.

*Corresponding author: mvalero@usal.es

Abstract

The present work examines the behavior of salicylic acid (SAL)-loaded F127 micelles as drug nanocarriers for controlled release by means of interaction with 2,6-dimethyl-β-cyclodextrin (DIMEB) in the intestine at basic pH=7-8, both important excipients, of pharmaceutical formulations.

The results show that acidic pH (pH=1) strongly increases the partitioning of SAL in F127 micelles compared to neutral pH, due to the drug being in its molecular form. Fluorescence spectroscopy and small-angle neutron scattering show that free and SAL-loaded F127 micelles transition to cylindrical micelles at pH=1 and high temperatures (37ºC). Micelles loaded with SAL are disrupted by DIMEB to a higher extent than at pH=7 at physiological temperature. This study reveals that F127 could be a valuable nanocarrier for intestine controlled release of SAL. Taken together, our results highlight the importance of water in the structure of the micelles and their interaction with DIMEB, and bring precious insights into the mechanisms that regulate drug loading and release in complex formulations.

Key words

ABBREVIATIONS
SAL: Salicylic acid
PPO: polypropylene oxide
PEO: polyethylene oxide
NR: Nile red
DIMEB: heptakis (2,6-di-O-methyl)-β-cyclodextrin
SANS: Small angle neutron scattering
CP: Cloud Point

Salicylic acid (SAL); Pluronic® F127; 2,6- dimethyl β-cyclodextrin (DIMEB); cylindrical micelles; controlled release; small angle neutron scattering (SANS), fluorescence spectroscopy.

1. Introduction

Pluronics are a family of tri-block co-polymers formed by two lateral hydrophilic polyethylene oxide chains (PEO), and a central hydrophobic polypropylene oxide block (PPO), (PEO)x-(PPO)y-(PEO)x. Pluronic F127, also known as poloxamer 407, is a member of the family with composition $(PEO)_{100}$-$(PPO)_{65}$-$(PEO)_{100}$. As other Pluronics, F127 forms core-shell micelles (CS-micelles) above its critical micelle concentration (cmc), with a hydrophobic central core formed of PPO chains surrounded by a hydrophilic shell, which comprises the PEO blocks. Pluronic F127 has been widely studied as a drug carrier and is approved by the FDA and the British Pharmacopeia as an excipient for drug delivery after oral administration. F127 has demonstrated attractive properties in the pharmaceutical field such as improvement of the oral bioavailability of drugs [1–5] and the ability to incorporate into membranes [6,7], increasing the efficiency of anti-cancer resistant drugs [1,8] owing to its ability to inhibits glycoprotein G [9,10]. In addition, Pluronic F127 can also be envisaged for topical formulations, since it forms gels close to body temperature [11–15].

Recently, we have investigated the ability of F127 to load drugs with varying chemical structures [16–18] and how their release can be modulated by the interaction with cyclodextrins, another well-known pharmaceutical excipient.

Cyclodextrins are cyclic oligosaccharides made of glucose units that present a truncated conical shape. They have an inner apolar domain formed by the ether groups. Their hydrophilic external edges are lined with primary and secondary alcohol groups protruding out of the inner cavity, which can be further modified to improve their solubility or functionality. This unusual cyclic structure with an apolar interior gives cyclodextrins the ability to form inclusion complexes with different chemical compounds, in particular drugs, or thread polymer chains in structures referred to as pseudopolyrotaxanes (PPRs) [19,20]. The methylated derivative of β-cyclodextrin (β-CD, a 7-glucose unit construct), namely, heptakis (2,6-di-O-methyl)-β-cyclodextrin (DIMEB) (Scheme 1), has been shown to modulate the micellization of a range of PEO-based micellar aggregates [21–23], including free and drug-loaded F127 micelles [16–18], inducing – in certain conditions – full rupture of the micelles and therefore releasing a payload. It is clear from our previous work that temperature, the specific chemical structure of the drug and its precise localization within the micelle can all modulate the interaction between the micelle and DIMEB, and hence the extent of micellar disruption [16–18].

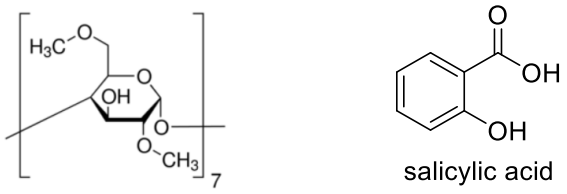

Scheme 1: Chemical structure of the basic unit of DIMEB (*left*) and salicylic acid (*right*).

However the rules that govern this modulation are still not understood; for instance, while the formation of PPRs as the lever that induces micellar rupture has been excluded, and possible external interactions between PO units and cyclodextrins envisaged instead [24], it is not clear how the presence of drugs in the micellar compartments modulate this interaction [17,18]. While it has now been shown that cyclodextrins can induce full demicellization, the control of the process under desired conditions is elusive. Therefore, an understanding of the mechanisms that underlie this process is needed to harness the potential of DIMEB in pharmaceutical formulations. Most of the studies carried out with F127, drugs and DIMEB were conducted at pH=7, but very few have been reported at acidic pH [16]. Following oral administration, drugs go through a range of pH in the gastrointestinal tract, ranging from 1 to 9, however very few studies have explored the behaviour of free F127 micelles at this pH [25], or other Pluronics [26–28]. The solubility of ionizable drugs varies considerably at this pH and compromise drug bioavailability [29]. Therefore, it is of interest to study the effect of acidic pH on these and other properties of F127, both free and loaded with acid-basic compounds.

Salicylic acid (SAL) (Scheme 1) is considered the most ancient remedy currently in use [30]. Recently, it has received great attention in the food and agriculture fields, since SAL is a hormone produced by some plants involved in the resistance against microbial pathogens and anti-cancer response [31]. It would therefore be potentially useful in human therapy against these pathologies, but the gastrointestinal side effects make its oral administration impossible. On the other hand, SAL is the only non-steroidal anti-inflammatory drug (NSAID) with a potent keratolitic activity [32] and therefore it is widely used in topical applications, both in cosmetics and dermatological consumer products. High drug concentrations are allowed in these formulations, up to 2% (w/w) for acne treatment by the Food and Drug administration, (FDA) [33], or up to 3% in leave-on and rinse-off, and in cosmetics such as face and general creams, shower gels, shampoos, etc by the Europe Cosmetics Regulation EC 1223/2009. Salicylic acid is absorbed through the skin from topical formulations; the percutaneous absorption is strongly dependent on the pH [34], but in most of the formulations cited above, the pH is not controlled. In this context, the development of new SAL formulations intended for oral and topical administrations is a worthy endeavour. For this purpose, we need a fundamental understanding of the effect of pH on loading capacity and solubilization locus and on how micellar morphology and properties are affected by the presence of the drug, and, in turn, by interactions with cyclodextrin used as a handle for drug release; this knowledge will help tailor formulations to desired outcomes.

Based on these considerations, the present work gives a detailed characterization of F127 micelles, free and loaded with the drug salicylic acid at pH=1, over a range of temperatures, in the absence and presence of DIMEB, which acts as a micellization-modulator. We use small-angle neutron scattering (SANS) to examine the morphology of the free and drug-loaded micelles under a range of conditions, in the absence and presence of DIMEB. Fluorescence and UV-Vis spectroscopies are employed to measure the partitioning of the drug withing the micelles, its binding to cyclodextrins, and shed light on the localization of SAL in the micelles, to bring an understanding into these complex three-way interactions (drug-micelles-cyclodextrin), which determine the state of aggregation of the drug nanocarrier and hence drug loading and release. Our results form the basis for a formulation rationale and highlight the importance of water in the interactions.

2. Experimental Section

2.1. Materials

Pluronic copolymer F127 comprising a central block of 65 PPO units and two side-blocks of PEO (100 units each) was obtained from Sigma-Aldrich UK (M_w = 12,600). Heptakis (2,6-di-*O*-methyl)-β-cyclodextrin (DIMEB) was obtained from Sigma-Aldrich UK (H0513, M_w = 1331.4 g mol^{-1}).

The drugs sodium salicylate (SAL, 71945) and salicylic acid (SAL, 84210), Nile red (NR, M_W 318.4 g·mol^{-1}), HCl (320331) ACS reagent, 37%, as well as D_2O (151882) with a purity of 99.9 %, were purchased from Sigma Aldrich. The aqueous solutions were prepared using Milli-Q water or D_2O as specified.

All materials were used as received.

2.1. Sample Preparation

Aqueous and D_2O stock solutions of sodium salicylate (1) alone, (2) with F127, and (3) with DIMEB, as well as (4) F127 alone, were prepared by weight. Aqueous and D_2O stock solutions of 0.2M HCl and DCl, respectively, were prepared. For partition coefficient determination by fluorescence, solutions of constant drug and different F127 concentrations were prepared by mixing the appropriate amount of solutions (1) and (2). Two regimes of drug concentration were studied: dilute ($1.5 \cdot 10^{-3}$ wt%) and concentrated, 0.16 wt%, limited by the aqueous solubility (S_0 < 0.2% (w/v) found for sodium salicylate at pH=1 and 25ºC.

For the determination of the CD-drug binding constant, solutions at constant drug and different CD concentrations were prepared by mixing solutions (3) and (1). In both cases, the required amount of DCl or HCl to achieve pH=1 was added.

For the determination of partition by uv-vis spectroscopy, a fixed amount of salicylic acid was weighed and a constant amount of F127 solution at different concentrations, prepared from solution (4), was added. After adding the amount of DCl or HCl needed to obtained the desired pH, the solutions were kept stirring over a week at room temperature. The pH of saturated solutions was corrected to achieve the same final pH in all the samples. The

excess of solid drug was removed by centrifugation. Samples were diluted and the pH corrected again before uv-vis absorption measurement.

For the determination of the critical micellar concentration (cmc), solution (2) was diluted to produce a range of F127 concentrations. The cmc value of F127 at pH=1 used to determine partition was obtained by dynamic light scattering (DLS) as cmc= 0.04 wt %.

A F127 molar volume of $\overline{V}$ =10.8 L/mol, was experimentally obtained by density measurements with a pycnometer, at room temperature.

Samples for cloud point measurement were prepared by weighting the appropriate amount of salicylic acid (and sodium chloride, when added), and further addition of the required amount of F127 (2) and DCl stock solutions, completing with D_2O. All solutions were prepared by weight and then most of the concentration units refer to weight %.

Appropriate volumes of concentrated NR stock solution in ethanol ($4.66 \cdot 10^{-3}$ M) were taken, to achieve a final NR concentration of $4.66 \cdot 10^{-6}$M, then the solvent was evaporated. The residue was then solubilized in either water, 5 wt% F127, or 5 wt% F127 1wt% SAL aqueous solutions at pH=1.

2.3. Methods

2.3.1. UV-vis absorption spectroscopy

The absorption spectra of SAL and NR were obtained in a Perkin Elmer UV/Vis spectrometer (Lambda 2).

The UV absorption of the drug was measured at λ=300 nm, corresponding to the isosbestic point for molecular and ionized SAL, using a Perkin Elmer UV/Vis spectrometer (Lambda 2). Solubility was determined using the molar absorptivity value, ε_{300}^{H2O}= 3550 M^{-1} cm^{-1} experimentally obtained. The increase in SAL solubility with F127 addition was quantified as the ratio $S_{0,F127}/S_{0,H2O}$, where $S_{0,F127}$ is the solubility of SAL at a given F127 concentration and $S_{0,H2O}$ the solubility of SAL in water.

All the experiments were carried out at 25ºC.

2.3.2. Steady- State Fluorescence spectroscopy

Measurements were performed on a Cary Eclipse fluorescence spectrophotometer (Varian, Oxford, UK).
The excitation wavelength used for salicylic acid was λ_{exc}= 296 nm. Emission intensity variation was followed at λ_{em}= =440 nm.
The binding constant of the drug to F127 micelles, $K_{F127,}$ was determined at two drug concentrations: $1.5 \cdot 10^{-3}$ wt% and 0.16 wt%, using the method proposed by Almgren [35] and the mathematically modified equation (Eq.1), as described elsewhere [18].

$$\left(\frac{F_0}{F-F_0}\right) = \left(\frac{F_0}{F_\infty - F_0}\right)\left(1 + \frac{1}{K_{F127} C_M}\right) \qquad \text{Eq. (1)}$$

where C_M is the micellized surfactant concentration with $C_M = (C_S - \text{cmc})$, C_S being the total surfactant concentration, F is the measured fluorescence intensity, F_0 and F_∞ are the fluorescence intensity when all the drug is free and complexed, respectively. K_{F127} is the binding constant of the drug to the micelle, obtained by fitting the experimental data. The critical micelle formation of F127 at pH=1, cmc = $4 \cdot 10^{-2}$wt%, estimated from dynamic light scattering (DLS) data, was used.

F_0 was obtained from experimental data, while F_∞ was obtained by fitting and further comparing to the experimental value as a control of the fitting model. The F_∞ value obtained from the fitting (y-intercept) reproduces reasonably well the experimental value of this parameter.

Plots of $F_0/(F-F_0)$ vs $1/C_M$ give a linear plot, where the ratio of the y-intercept over the slope gives K_{F127}.

The concentration of F127 was expressed in mass fraction (X) for consistency of units between all experiments; as a result, the binding constant, which is expressed in inverse of concentration units, X^{-1}, is given in g/g.

The partition coefficient, P, can be calculated from the binding constant, K_{F127}, using Eq.(2) [36] as previously reported [17].

$$K_{F127} = (P-1)\ \bar{V} \qquad \text{Eq. (2)}$$

where K_{F127} is the binding constant of SAL to F127, M^{-1} (conversion from X^{-1} was made using δ_{F127}=1.0099 g/mL, obtained experimentally at 25ºC); $\bar{V}$ is the partial molar volume of F127 ($\bar{V}$ =10.8 L/mol, experimental value).

The binding constant of the drug ([SAL] = $1.5 \cdot 10^{-3}$ wt%) to the cyclodextrin, K_{DIMEB}, was determined as described previously [17,18] by fitting fluorescence intensity at λ=440 nm, to Eq (3).

$$F = \frac{(F_0 + F_\infty K_{DIMEB}[CD])}{1 + K_{DIMEB}[CD]} \qquad \text{Eq. (3)}$$

where F is the measured fluorescence intensity, F_0 and F_∞ are the fluorescence intensity when all the drug is free and complexed, respectively; both of them are experimental values. [CD] is the concentration of free cyclodextrin, which, in these dilute systems, corresponds to the analytical concentration, since [CD] >> [drug]. A non-linear least squares method was used to fit the experimental results to Eq (4) and obtain K_{DIMEB}. The [CD] concentration used was expressed in mass fraction (X) for consistency of units between all experiments; as a result, the binding constant, which is expressed in inverse of concentration units, X^{-1}, is in g/g.

Both studies were carried out using H_2O as a solvent. For comparative purposes, some experiments were also performed in D_2O.

2.3.3. Small-Angle Neutron Scattering (SANS)

SANS experiments were carried out on the KWS-2 diffractometer at the Jülich Centre for Neutron Science (JCNS), Münich, Germany [37]. An incidental wavelength of 5 Å was used with detector distances of 1.7 and 7.6 m and a collimation length of 8 m, to cover a momentum transfer, q, range from 0.008 to 0.5 $Å^{-1}$. In the standard mode, a wavelength

spread $\Delta\lambda/\lambda$= 20% was used. All samples were measured in quartz cells (Hellma) with a path length of 2 mm using D_2O as the solvent. The samples were placed in an aluminium rack where water was recirculated from an external Julabo cryostat, at 20-50ºC. This set-up enables a thermal control with up to 0.1 ºC precision. Scattered intensities were corrected for detector pixel efficiency, empty cell scattering and background due to electronic noise. The data were set to absolute scale using Plexiglas as a secondary standard. The obtained macroscopic differential cross-section $d\Sigma/d\Omega$ was further corrected for contribution from the solvent. The complete data reduction process was performed with the QtiKWS software provided by JCNS in Garching [37].

Solutions of F127 5 wt% with 1 wt% salicylate sodium salt at pH=1 were prepared. DIMEB concentrations, when added, ranged from 5 to 11 wt%. All samples were measured in D_2O to optimize the contrast and minimize the incoherent background for SANS experiments.

SANS curves, after subtraction of the background, were fitted using SAS View 4.2.1. software [38] to a core-shell sphere model (CSS) [39] (curves at 20-37ºC) or core-shell cylinder (CSC),[40,41] (curves at 37 and 50 ºC), which were combined to a hard-sphere (HS) structure factor. Except in SAL-loaded F127 micelles at 50ºC, a contribution of random coils, with R_g=7-12 Å, from PEO, was considered, as in previous work [18,42]. The size polydispersity of the micellar core, shell thickness and length (for the CSC) were fixed for each set of data to minimize the number of fitting parameters to: 0.15/0.20 (C/S) at 20-37ºC (CSS) and 0.15/0.2/0.1 (C/S/L) at 37 and 50 ºC (CSC). In the SAL-loaded micelles, polydispersity was fixed to 0.15/0.15 at 20, 25 ºC; 0.10/0.20 at 37 ºC, (CSS); and 0.10/0.20/0 at 37 and 50 ºC (CSC).

The curves of SAL-loaded micelles in the presence of DIMEB were fitted to a core-shell sphere (CSS)[39] with additional spheres of R = 9 Å to account for DIMEB (5% DIMEB) or poly-gaussian coils R_g=11 and 13Å (at 7 and 9 wt% DIMEB, respectively). With 11 wt% DIMEB, a poly-gaussian coils model [43–45], with a sphere contribution (R = 32 Å) was used. The scattering length density of DIMEB was fixed at $sld_{DIMEB}=1.89 \times 10^{-6}$ Å^{-2}. The size polydispersity was fixed at 0.16 in all cases.

In order to reduce the number of fitting parameters, in all the fits, the sld of the core was initially fixed at $sld_{PO} = 0.4 \times 10^{-7}$ Å^{-2}, reflecting a very dehydrated core, as observed for other poloxamines, [17,18,21,46,47]. This value was kept constant at temperatures 20-37ºC, but at 37 and 50 ºC it was a floating parameter.

The water content of each part of the aggregate was determined from the corresponding sld returned by the fits from Equation (4).

$$sld_{core/shell} = X_{PPO/\,PEO} \times sld_{\,PPO/\,PEO} + X_{D2O} \times sld_{\,D2O} \qquad \text{Eq. (4)}$$

with sld_{PPO}=4x10^{-7} or the value obtained from the fits (see above); $sld_{PEO}= 6.70 \times 10^{-7}$; $sld_{D2O}= 6.36 \times 10^{-6}$.

2.3.5. Cloud Point (CP) determination

Cloud points were determined by visual observation of the turbidity of the samples (in 1.5 mL eppendorf) immersed in a water bath. The temperature was increased by 1ºC intervals up to phase separation. All measurements were made in triplicates.

3. Results and Discussion

3.1. Salicylic acid partition and binding constant to F127 micelles

Initially, the partition of SAL, both in molecular and ionized form, in F127 micelles, was determined from solubility data at 25ºC in water and at different F127 concentrations, by UV-vis absorbance spectroscopy [48], over a range of pHs, therefore in systems containing varying fractions of ionized and unionized ("molecular") SAL.

The solubility of SAL increases with F127 concentration at all pHs studied (supplementary material, SI 1). $S_{0,F127}/S_{0,H2O,}$ at 5% F127, is higher at pH values below the pKa (pKa = 2.97 [49]), where the non-ionized form of the drug is present in higher amounts, in very good agreement with a higher solubilisation of the molecular form of the drug, rather than the charged (anionic one) in the micelles.

The solubility ratio $S_{0,F127}/S_{0,H2O}$ increases linearly with the volumetric fraction of F127 (Figure 1A). The slope of the curves increases as the pH decreases, reflecting a higher partitioning of the molecular vs. the ionized form present in the system at each pH. A linear fit of these plots at different values of the pH against the ionization percentage (Figure 1B) enables an extrapolation of the partition to 0% and 100% ionization, corresponding to the molecular and ionized forms of the drug, respectively. The results obtained are P = 115.7, logP =2.1 (logP=2.3 in octanol/water [50]), for molecular SAL, and P = 5.5, logP=0.74, for ionized SAL (P=-1.36 in octanol/water [51]. A very good agreement of the molecular partition with that in octanol/water is found; in contrast, the partition of ionized SAL is much higher than in octanol/water. This effect has been recently observed in the case of naproxen loaded in SDS micelles (Valero 2020, under review). In both cases, despite the low dielectric constant of the environment, the presence of water in the micelles could facilitate partition compared to octanol. This result shows that F127 is able to efficiently load salicylic acid present at pH=1 in the stomach, in contrast to ionized salicylate, present at pH values above the pKa, which showed lower partition [18].

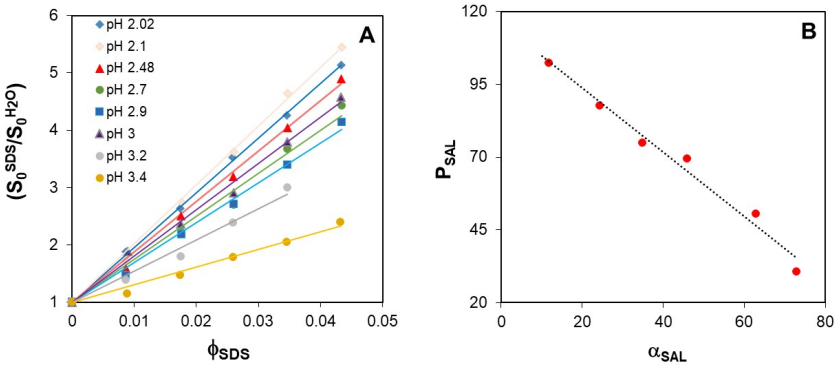

Figure 1. A: Change of SAL solubility with F127 volume fraction, at different values of pH; B: SAL partition (P_{SAL}) against ionization degree of SAL (α_{SAL}) in H_2O at 25ºC.

In order to compare the partitioning at pH=1 and pH=7, the binding constant of SAL to F127 at pH=1 was also obtained by fluorescence spectroscopy, using a method previously used for ionized salicylate as sodium salt [17,18]. In this case, the emission spectrum of SAL in the presence of increasing amounts of F127 was obtained and the variation in emission intensity (λ_{em}= 440 nm) with polymer concentration (Fig.2A) was fitted to Eq. (1) (Fig.2B).

.

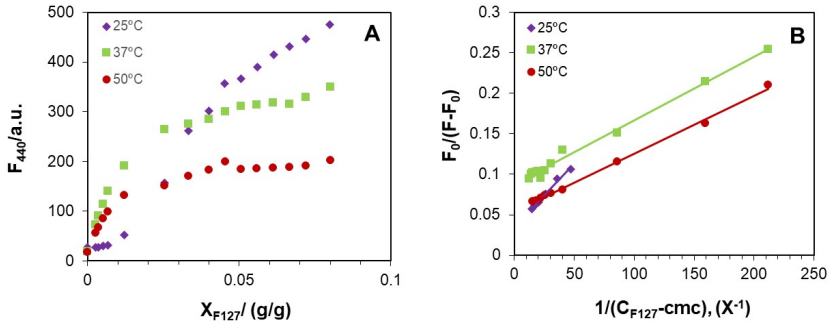

Figure 2: A: Change in fluorescence intensity at λ_{em}=440 nm for 0.16 wt% SAL in H_2O in the presence of increasing amounts of F127, at 25º C (diamonds), 37º C (squares) and 50º C (circles). B: fitting of the data to Eq.(1).

The results shown in Table 1 show a higher partition at pH 1, compared to pH 7, despite the higher drug concentration used (2% wt) at neutral pH compared to acidic pH (1 wt%).

	K_{F127} /X^{-1}(g/g)/ Diluted			*K_{F127} /X^{-1}(g/g)/ Concentrated*		
pH	*298K*	*310K*	*323K*	*298K*	*310K*	*348K*
1 (H_2O)	7.4±0.07	77.6±0.15	110±0.51	71±0.07		
7 (H_2O)	No detected*	No detected**		4.55±0.32*	18.3±0.3**	
1 (D_2O)	10±0.41	107.5±0.25	74.3±0.52	78±0.30	116±0.36	79±4.58

***** data reproduced from [17]; ****** data reproduced from [18].

Table 1. Binding constant K_{F127} (g/g) of sodium salicylate to 5 wt% F127 Pluronic micellar solution in H_2O and D_2O at pH=1, at different temperatures, determined from the variation of F_{440} with surfactant concentration using Eq (1). Two drug concentrations are studied: diluted (C_{drug} = 1.5×10^{-3} wt%) and concentrated (C_{drug} = 0.16 wt%). For comparative purposes, the results obtained in H_2O at pH=7 are included; in this case SAL concentrations were 1.5×10^{-3} wt% and 2 wt%.

The partition of molecular and ionized SAL obtained from absorption and emission spectra, at high drug concentration and 25ºC, were compared. For this purpose, partition (P) was determined from the binding constant obtained from fluorescence using equation (2). The binding constant (K_{F127}) of salicylate anion to F127 was found to be $K_{F127} = 4.55$ X^{-1} (X^{-1}: inverse of concentration in g/g) [17] (K_{F127}= 56.8M^{-1}), which gives P = 6.3 (log P=0.80) for the partition of the anionic form; this value is in very good agreement with the value of P=5.5 (log P=0.74) obtained by absorption spectroscopy. In the case of molecular SAL, K_{F127}=71 X^{-1} (Table 1) (K_{F127}= 886 M^{-1}), which gives P = 83 (log P=1.9). The larger difference obtained for molecular salicylic acid partition (P = 83 vs. P = 115.7) with both techniques, arises from the difference in the drug concentration used: in fluorescence, the working concentration of SAL is limited by its aqueous solubility, whereas in UV-vis absorbance it is the solubility in F127 micelles, hence the higher partition obtained by absorption can be attributed to the higher drug concentration, as usually observed [17,18,52,53].

Finally, and in order to reproduce the conditions used in the study of micellar morphology by SANS (see further down), the partition was also obtained in D_2O, at 25, 37, and 75 ºC at both SAL concentrations. As can be observed (Table 1), partition is not affected by the solvent (H_2O vs D_2O); it increases with temperature and drug concentration as observed in water [17,18,29,52,53].

Overall, the number of drug molecules inside the aggregate at pH=1 is much higher than at pH=7, in agreement with the absence of charge at low pH and the lower aqueous solubility. No major differences are observed in the partition of the drug in H_2O and D_2O.

The emission spectrum of SAL is sensitive to changes in the properties of the environment in which it is solubilized [54–56]. These changes could provide valuable information about the local compartment where SAL is solubilized in the micelles, as well as the interaction of the drug with the aggregates. Therefore, in addition to partition, we next study the changes in fluorescence spectra of SAL in D_2O under different conditions.

3.2. Photophysical behavior of salicylic acid loaded in F127 micelles

SAL emission spectrum is known to show two bands, the band in the UV region is referred to as the U-band (appearing in the range λ_{max}=340 - 370 nm), and the another in the blue region is known as the B band (appearing in the range λ_{max} = 380 - 480 nm)[57]. SAL species emitting at each band could be different depending on the medium in which the drug is solubilized, in this case water or the micelle. Salicylic acid in polar solvents is present as different ionized species (monocation, monoanion and dianion), whereas in its non-polar form it dimerizes at moderate concentrations [56]. In addition, in the excited state, SAL undergoes intramolecular proton transfer (excited state intra-molecular proton transfer, ESIPT), between the carboxylic ketone and the adjacent hydroxyl group giving rise to a cycle. In general, non ESIPT species of SAL emit in the U band, whereas species undergoing ESIPT emit at B band. Depending on the emissive species present under different conditions, the emission spectra of the SAL, shape, intensity and maxima position, could be modified.

The emission spectrum of 1.15×10^{-3} wt % SAL in D_2O (Fig 3A) shows a main band (λ_{max}= 436 nm) and a shoulder (λ_{max}= 360 nm); the main band is centered between that of the monocation (λ_{max}= 407 nm), expected to be present at the working pH, and the zwitterion (ESIPT species) appearing in methanol at acidic pH (λ_{max}=450 nm) [55]; it suggests that the spectrum corresponds to the emission of a mixture of both species: the monocation emitting at a lower wavelength (U band) and the neutral SAL (ESIPT) emitting at high wavelength (B band). At 0.16 wt % of SAL (Fig. 3B), a main band (λ_{max}=415 nm), with a less pronounced shoulder is present in the spectrum. The position of the main band (λ_{max}=415 nm) is also red-shifted compared to that of SAL as a monocation (λ_{max}= 407 nm), suggesting the presence of some neutral form (ESIPT). The protonation equilibrium seems to be shifted towards the neutral form in diluted system but towards the monocation in the concentrated one, perhaps due to a lower pH produced by the presence of higher amounts of SAL.

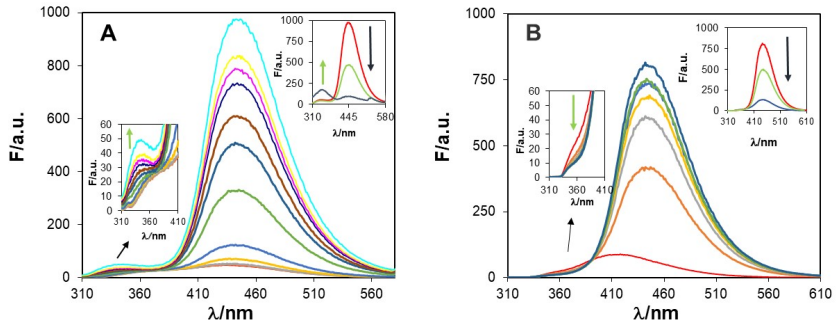

Figure 3: Emission spectra of SAL in the presence of increasing amounts of F127 (0-5 wt%) in D_2O at different temperatures **A:** diluted 1.5×10^{-3}wt% SAL. **B:** concentrated 0.16wt% SAL. *Insets left*: change in the emission intensity of U (340 nm) band with F127 concentration; *Insets right up*: fluorescence spectra of SAL loaded F127 micelle at 25ºC (brown), 37ºC (green) and 75ºC (blue).

The addition of F127 produces a strong increase in the emission intensity and a red shift of the main band of the spectrum (Figure 3) from λ_{max}= 436 or 415 nm in D_2O (diluted and concentrated SAL respectively) to λ_{max}=445.5 in F127 (B band), at both drug concentrations. In general, shifts in the maximum of the bands of the spectra are related to changes in the polarity of the local environment. In addition, the increase in the emission intensity shows a decrease in deactivation processes of the excited state. Non-radiative deactivation of SAL dissolved in polar alcoholic solvents decreases as the viscosity of the alcohol increases [55]. Therefore, these changes show that SAL is transferred from the polar D_2O to the apolar micellar environment, in good agreement with SAL partition. The maxima position shows that in the micelle the SAL is mainly in its neutral form undergoing ESIPT (λ_{max}=450 nm) [55], at both drug concentrations.

At pH =7, the maxima position (λ_{max} = 410 nm [17]), appears strongly blue-shifted and presents a higher emission intensity than in acidic conditions, characteristic features of the deprotonated salicylate anion [57–59]. Partition of SAL in F127 micelles produces a

quenching of the fluorescence of the emission band [17], due to the proton transfer from the water to the ionized carboxylic hydroxyl group of the anionic SAL inside the micelle, as observed in a poly (vinyl alcohol) matrix [60] and in dioxane and acetonitrile water mixtures [58]. This behavior agrees with the increase in the emission intensity when SAL partitions at pH=1 and the existence of only the deprotonated ESIPT in the micelle. Inclusion in cationic micelles of cetyl (CTAB) [61] tetradecyl (TTAB) [59] trimethylammonium bromide produced an increase in the fluorescence in good agreement to non protonation of the salicylate due to the interaction with the positive charge of the surfactant, which produces a growth of the micelles [59,61] even in microemulsions [62].

The intensity of the B band decreases with temperature at both drug concentrations, (Fig. 3A and B, *Insets right*), which shows temperature promotes some non-radiative deactivation mechanism. The vibrational deactivation of the excited state of the emissive species, due to a decrease in viscosity with temperature, is well known in homogeneous media [55]. In contrast to the homogeneous media, the micelle size increases with temperature [18], so the micelle inside is expected becomes more viscous.

By contrast to the B band, in the presence of F127, the U band, appearing in bulk D_2O, undergoes different changes depending on drug concentration. At 1.15×10^{-3} wt% ($\sim10^{-4}$M) SAL concentration, its intensity increases with F127 concentration (Figure 3A, *Inset left*); hence, inside the micelles, there is a SAL species, without ESIPT, emitting at this band (λ_{max}= 340 nm). This emitting species is promoted by temperature, as this the main band at 75ºC (Figure 3A, *Inset right*). The emitting species at the U band in non-polar media, it has been usually assigned to dimers without ESIPT [54,55,63,64]. However, dimers were detected in cyclohexene at drug concentration, 10^{-5}M, lower than in the present case, the increase in temperature decreases the amount of dimers [56], so a decrease in the U band with temperature would be expected. Although the effect of temperature on the micelles could be different to homogeneous media, the presence of other species other than dimers must be consider (most probably, the cation detected in bulk D_2O).

At higher SAL concentration, 0.16 wt % (1.16×10^{-2}M), the intensity of the U band appearing in D_2O (Figure 3B, *Inset left*) decreases as F127 concentration increases and SAL is transferred from water to the micelles, consequently, the emitting species without ESIPT, emitting at the U band, is not present when the drug is completely inside the micelle. The U band is not present in the micelle at any temperature studied at this drug concentration (Figure 3B, *Inset right*). Therefore, in the concentrated system, only the ESIPT emitting species exists. The same feature was described in the 10^{-3}M SAL in a poly (methyl methacrylate) polymer matrix, PMMA. It was related to intermolecular hydrogen bonding of SAL, through the carboxylic hydroxyl group and the polymer [55] which strengthen the intramolecular one, ESIPT [54], promoting the species emitting at B band over the U one (assigned in this study to a dimer, the most expected species in non-polar media).

Since the photophysical behavior of SAL is governed by protonation, the behavior observed with drug concentration and temperature at pH=1 could be explained on the basis of different protonation of the carboxylic hydroxyl group. In the micelle, the same species are present, namely, the monocation and neutral form (ESIPT). The micelle is more efficient as a proton donor at low drug concentration (presence of U band) and at high

temperature (quenching of B band at both drug concentrations and in diluted systems the appearance of the U band).

Despite the micellar core location of the drug demonstrated before by NMR [18] and the possibility of forming inter-molecular hydrogen with PPO groups of F127 in the micelles as observed in mixtures of F127 with polyacids [25], the results point to a different hydration of the drug inside the micelles at the origin of the effects observed with concentration and temperature at pH=1, as reported recently for other compounds [65], as well as for the anionic salicylate in a poly (vinyl alcohol) matrix [60] and in mixtures of solvents with water [58]. In these studies, water clusters act as proton donors to the salicylate anion, resulting in a quenching of fluorescence. Interestingly, quenching of fluorescence produced by water was demonstrated to be dependent on the size of the water cluster, being operative at high water content ($x_{H2O} \geq 0.8$) in dioxane/water mixtures [58].

In order to obtain information about the water content in the free and loaded micelles, we next checked the polarity of the core of the aggregates by UV-absorption using Nile Red as a molecular probe.

3.3. Nile Red as a probe of the polarity and water content of the micelles

Nile red (NR) is a fluorescent probe that presents a high sensitivity to the polarity of the medium [66–68] and therefore to the presence of water. The absorption and emission maxima of the probe are red-shifted when it is transferred from a non-polar to a polar medium [69,70]. NR and SAL absorption spectra do not overlap, making this probe a suitable candidate to examine the water content of the micellar region of the aggregate where it is located, in both the free and the SAL-loaded F127 micelles.

The absorption spectra of NR in H_2O, 5 wt % F127 and SAL:F127 (1:5 wt%) at pH=1 are shown in Figure 4. In water, NR shows a low absorbance band centred at λ_{max}=594 nm. The addition of F127, in both cases, produces a strong hyperchromic effect (Figure 4), besides a blue shift in the maximum λ_{max}=544 nm and λ_{max}= 562 nm in the absence and presence of SAL, respectively. These changes show that NR, in both cases, is being transferred from the bulk water to a less polar media, that is, inside the micelles. The strong red shift of the NR maximum position when partitioned inside the micelles, in the presence of drug, points to a higher polarity in SAL-loaded micelles than in the free micelles. Therefore, in contrast to what was speculated in the previous section, NR points to a higher water content of the SAL-loaded micelles than in the free micelles.

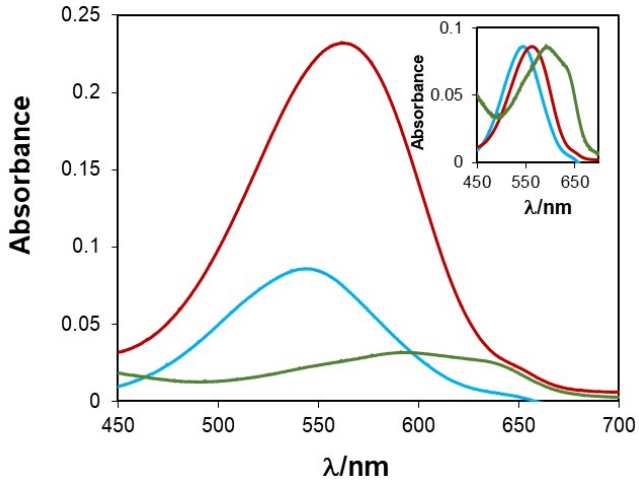

Figure 4: Nile Red 4.66×10^{-5}M: **A:** UV-vis absorption spectra in H_2O (green), 5% F127 (Blue) and SAL1% F127 5% (dark red), pH=1. *Inset*: Shift of these bands by manipulation of the bands to show them on a comparable scale (multiplying and dividing by 2.7, in water and SAL loaded system, respectively).

A rough estimation of the polarity of the microenvironment where the probe is dissolved can be obtained by comparing the maxima position of NR in the micelle to that in a medium of known dielectric constant. In the free micelles at pH=1, λ_{max}=544 nm, the polarity is between acetone (ε=20.7, λ_{max}=536 nm) and EtOH (ε =24.5, λ_{max}=554 nm)[71], or between dichloromethanol (ε=8.93, λ_{max}=538 nm) and acetonitrile (ε=37.5, λ_{max}=556 nm)[72]. Hence NR in the micelles would be in a medium with a dielectric constant around ε = 23 (obtained as a mean value of the dielectric constants of homogeneous media with similar absorption maxima).

If we consider that only PPO or PEO and water are contributing to the polarity, the dielectric constant of the micellar core may be related to the water content by equation 5:

$$\varepsilon = X_1 \times \varepsilon_1 + X_{H2O} \times \varepsilon_{H2O} \qquad \text{Eq. 5}$$

where X_1 is the fraction of PPO or PEO in the micelle, depending if the probe is in the core or the shell, respectively; ε_1: is the dielectric constant of PPO or PEO depending if the probe is in the core or the shell, respectively. The dielectric constant of propylene oxide is ε=16 [73] and ethylene oxide ε=13 [74].

The water content obtained for the micellar compartment where the probe is located would be 11% (considering ε of PPO and PEO, respectively). These values are far from the shell water content, which usually is higher than 90% [18], pointing to a core location of NR; the value of 11% is in very good agreement with the value of 10% reported for F127

519 micelles (3 %) [75], or 17% for 1% F127 at 37ºC [42] and other Pluronics [76,77] obtained
520 by SANS.

521 In the SAL-loaded micelles, NR absorption maximum is λ_{max}= 562 nm, suggesting a
522 dielectric constant higher than in acetonitrile (ε=37.5, λ_{max}=556 nm) [72], which gives a
523 water content as high as 33.5% for the locus of the probe in the loaded micelle. This value
524 is higher than values usually detected, however, in certain cases the volume fraction of
525 water in the core can be as much as 40%, for example in P85 at 50-60ºC, obtained by
526 SANS [76].

527 The higher water content in the loaded micelle suggests that SAL retains water, in good
528 agreement with intermolecular hydrogen bond formation, as suggested by fluorescence,
529 but with the water molecules instead of with the PPO groups of the F127 core. On the
530 other hand, this value could be overestimated due to the increase of the polarity of the core
531 due to the presence of SAL itself [27]; in this case, a third term - corresponding to the drug
532 contribution - should be included in Eq. 6, resulting in a lower value of the water content,
533 or it could be that the drug promotes NR solvation inside the micelles [78].

534 Next, the effect of the presence of molecular SAL on the structural features of the micellar
535 aggregates was investigated by SANS.

536

537 *3.4. Small Angle Neutron Scattering of free and SAL-loaded F127 micelles*

538 In this section, the effect of the presence of SAL on the micellar structure, with and without
539 DIMEB, is examined at different temperatures.

540

541 *3.4.1. Effect of acidic pH and temperature on F127 micelles*

542 SANS curves of free and SAL-loaded F127 micelles, at pH=1, were obtained over a range
543 of temperatures (20 to 50ºC) (SI 2) and fitted to different models (Figure 5).

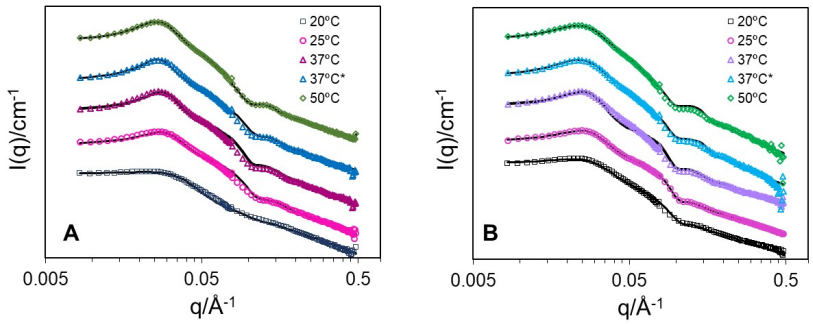

544
545 **Figure 5:** Small-angle neutron scattering curves from A: free and B: SAL (1 wt%) loaded
546 F127 (5 wt%) micelles at pH=1, at different temperatures, from 20 to 50 ºC. The curves
547 have been staggered for better visibility. Solid lines correspond to fits to CS-spheres (20-
548 37 ºC) or CS-cylinder (37 ºC*, 50 ºC), combined with a hard sphere structure factor, at
549 different temperatures.

The data were fitted by a core-shell sphere or cylinder model with a hard-sphere structure factor. The most important change in both free and loaded micelles is that temperature promotes the structuration of the micelles, with the reinforcement of the peak in the scattering curves, which reflects the presence of interactions. In addition, at high temperatures, we observed an elongation of the micelles (Tables 2, 3). At 20 and 25 ºC, the curves are well described by a spherical core-shell model; at 37ºC, they can be fitted both to spheres and cylindrical aggregates, with the latter giving better fits; at 50 ºC, only the core-shell cylinder gives suitable fits, suggesting a transition from sphere to rods with temperature. The presence of SAL in the micelles seems to promote this elongation at lower temperature (37 ºC), leading to longer micelles at 37 ºC (151 vs. 106 Å in the absence of drug) (Tables 2, 3), and of similar length at 50 ºC (153 vs. 150 Å) (Tables 2, 3). Therefore, a combination of low pH, high temperature and presence of SAL seems to promote micellar growth. No data about the effect of acidity on free or loaded F127 micelles was found in the literature. Micellar growth was not observed at neutral pH over the range 30-50 ºC [79], or in the SAL-loaded micelles at 37 ºC [18]. In agreement with these findings, paclitaxel, an anti-cancer drug, was found to induce micelle agglomeration and a shape transition of F127 to cylindrical micelles over the temperature range 37-50 ºC [80]. In mixtures of F127 with poly (aspartic acid), the formation of cylindrical micelles was also suggested on the basis of viscosity measurements [25]. A sphere-to-rod transition of F127 has also been observed upon approaching the cloud point in the presence of NaCl and butan-1-ol [81]. Cylindrical micelle formation has also been described for smaller Pluronics such as P85 loaded with SAL at pH=1 [27], or P123 and P103 loaded with salicylic derivatives (methyl-salicylate and acetyl salicylic) at pH=7 [82], in both cases at 25 ºC. P105 loaded with glucose was also shown to form ellipsoid micelles at 55-60ºC [83]. The origin of this shape transition is not clear; in some cases shell dehydration has been invoked [27,83,84], but in other studies micellar growth was assigned to core dehydration [81,82].

T/ºC	*Core Radius Å*	*Shell Thickness Å*	*Length Å*	*Volume fraction*	*%D_2O core*	*%D_2O shell*
20	34	47	-------	0.12	41	94
25	37	61	-------	0.22	0	94
37	40	65	-------	0.29	0	92
37*	34	52	106	0.29	17	94
50	36	44	150	0.25	23	93
25	40	58	-------	0.14	0	90
37[a]	45	64	-------	0.25	0	92

[a] data reproduced from [18]

Table 2: Fitting parameters obtained from SANS curves of F127 micelles (5 wt%) at pH=1 in D_2O described by CS-spheres (20-37 ºC) or CS-cylinders (37*, 50 ºC), combined with a hard-sphere structure factor, at different

temperatures. For comparison, the last two rows include the data collected at pH=7, at 25 and 37 ºC [a], fitted to CS-spheres with a hard-sphere structure factor.

T/ºC	*Core Radius Å*	*Shell Thickness Å*	*Length Å*	*Volume fraction*	*%D_2O core*	*%D_2O shell*
20	39	61	-------	0.13	0	94
25	40	65	-------	0.20	0	94
37	43	66	-------	0.27	0	90
37*	38	48	151	0.28	33	94
50	39	45	153	0.26	35	92
25 [a]	35	52	-------	0.13	0	96
37 [a]	41	64	-------	0.26	0	92

[a] data reproduced from [18]

Table 3. Fitting parameters obtained from SANS curves of F127 micelles (5 wt%) loaded with SAL (1 wt%) at pH=1 in D_2O described by CS-spheres (20-37 ºC) or CS-cylinders (37*, 50 ºC), with a hard-sphere structure factor, at different temperatures. For comparison, the last two rows include the data collected at pH=7, at 25 and 37 ºC [a], fitted to CS-spheres with a hard-sphere structure factor.

We next turn our attention to the water content in the two compartments [85] of the micelles (core and shell). First, the shell of both free and SAL loaded micelles is highly hydrated (Tables 2 and 3), as observed for Pluronics and other PEG-base copolymers [18,85]. No meaningful change in the water content of the shell is observed with temperature (94% at 20ºC and 93 - 92%, at 50ºC), the presence of SAL (94% at 37ºC for both systems or 93- 92% for free and SAL loaded aggregates, respectively at 50ºC) or with pH (free micelles: at 25ºC 94/90% and at 37ºC 94/92% at pH=1/pH=7; or in the loaded micelles: 94/96% and 94/92% at 25 and 37ºC, pH=1/pH=7, respectively). This would suggest that hydration of the shell is unlikely to be playing a key role in micellar growth; however neutrons are not very sensitive to this region of the micelles (in particular to the chains further away from the aggregates).

In order to minimize the number of floating parameters, and based on previous studies of similar polymers [18,85], the water content of the core was initially fixed to zero, in other words, the scattering length density was fixed to the value of PPO (0.4×10^{-6} $Å^{-2}$). However, this assumption does not allow the fitting of the curves at all temperatures. In the free micelles, at 20ºC, the amount of water in the core was found to be quite high (41%), a value that is in good agreement with reported values of 37% or 40% for P123 in D_2O with 1.6M HCl at this temperature [77]; the water content is known to increase as temperature decreases [86] due to the higher polymer solubility and the formation of large

pre-aggregates [87]. In contrast to the free micelles, at this temperature (20ºC), SAL-loaded micelles can be fitted by considering a fully dehydrated core, suggesting that the micelle are fully formed (not pre-aggregates), suggesting that the presence of drug promotes micelle formation at lower temperatures. At 25 ºC, the curves of free and SAL-loaded micelles could all be fitted without water in their core. However, at 37º and 50ºC, when cylindrical micelles are formed, the presence of water in the core needs to be accounted for in all the micellar systems studied. In order to check the water content, the values obtained for the cylindrical micelles model were used. In free 5% F127 micelles, we obtained 17 and 23 % at 37 ºC and 50 ºC, respectively. These values are in good agreement with the value of 11% found for the free micelles at 25 ºC with the NR (previous section) and 17% obtained for 1 wt% F127 micelles at 37ºC [42], or around 20% for P123 micelles at 40ºC [77].

In the presence of SAL, the water content in the core is double that of the free aggregates: 33 and 35% at 37 and 50 ºC, respectively. The value at 37 ºC is in very good agreement to the one obtained by fluorescence with NR at 25ºC, reinforcing the idea of water retention by the drug and strong hydration of SAL in the aggregates' core. The water content of the core tends to increase with an increase in temperature in the free and SAL-loaded micelles; this effect was not observed with P123 in HCl [77]. On the other hand, EO groups tend to associate to protonated water molecules (H_3O^+) through the ether group [87]. Hydrogen bond formation between polyacids and ether groups, both with the PEO and PPO blocks of F127, has also been demonstrated [88]. Hence the protonation of the polymer chains and the presence of SAL seem to promote the presence of more water molecules in the aggregates as temperature increases.

Overall, therefore, core dehydration does not seem to be a driving force for micellar growth, since hydration seems to increase with temperature. What is changing in the systems under these conditions?. Looking at the features of free and SAL-loaded F127 micelles at pH=1 (Tables 2, 3), it is possible to make three observations. First, we observe the size of the core slightly increases with temperature. In the presence of SAL, the core is slightly swollen compared to the free micelles, at all temperatures, in agreement with the core location of the drug [18], as observed with other anti-inflammatory drugs [26,89]. Second, if we observe the thickness of the shell, this value increases with temperature in spherical micelles (47 to 65 Å or 61 to 66 Å in free and loaded micelles, from 20 to 37ºC), then drops sharply with the transition to cylinders and decreases with temperature as cylindrical micelles grow (from 61 to 44 Å (F127) and 65 to 45 Å (SAL:F127), from 25º to 50ºC, respectively).

Overall therefore, the data show that when the micelles grow (pH=1, T=37 and 50ºC the shell shrinks slightly, and the core accommodates higher amounts of water, which would result in more space between the hydrophobic chains. In summary, at pH=1 and high temperature, free and SAL-loaded micelles form highly hydrated cylindrical micelles.

Next, we check whether SAL-loaded F127 micelles are protected against the disruptive effect of DIMEB at pH=1, in such a way that the drug could remain encapsulated in the micelles under gastric conditions.

3.4.2. Interaction of SAL-loaded aggregates with DIMEB

SANS curves were obtained in the presence of 5, 7, 9 and 11 wt% of DIMEB at 20, 25, 37 and 50 ºC (Figure 6).

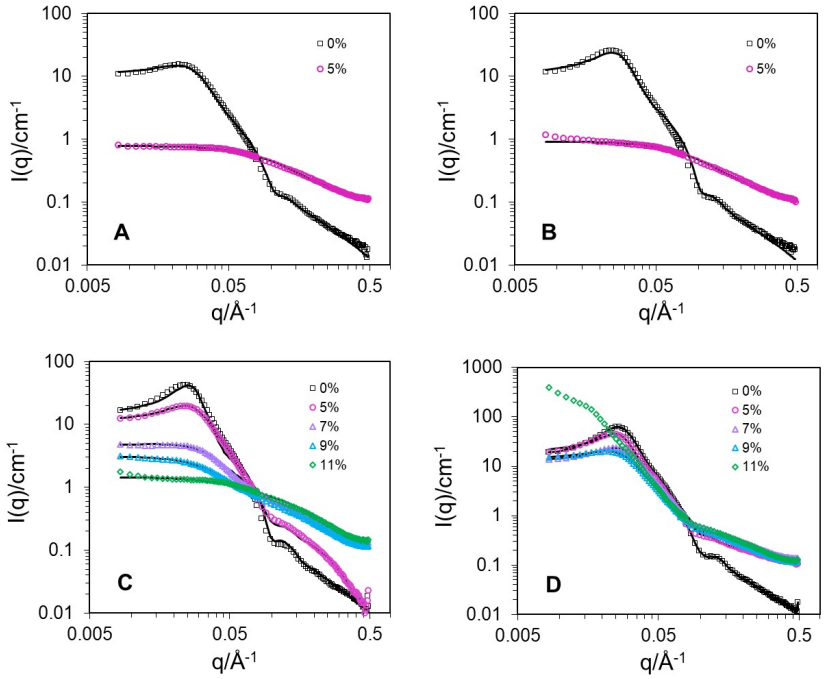

Figure 6: Small-angle neutron scattering curves of SAL (1%)-loaded F127 (5%) micelles at pH=1 in the absence (□) and presence of 5% (○), 7% (△), 9% (△) and 11% (◊) of DIMEB **A:** 20 ºC; **B:** 25ºC; **C:** 37 ºC; and **D:** 50ºC.

At 20 ºC (Figure 6A) and 25ºC (Figure 6B), the scattering curves are well fitted to Gaussian coils (fitting parameters included in SI 3) at the lowest concentration of DIMEB (5wt%), showing that SAL-loaded micelles are completely broken-up by the addition of 5 wt% DIMEB. At pH=7 and 25ºC (SI 3 and 4), the same amount of DIMEB is necessary to break up of the SAL-loaded micelles. In this case, salicylate partition is very low at this temperature and the presence of the charged drug reduces the size of the aggregates [17]. The fact that SAL-loaded micelles are not protected against the action of DIMEB with the high partitioning is observed (Section 3.1.) is unexpected, since in our previous [16–18] of drugs has been found to afford some protection against the disruptive effect of DIMEB. Hence, on the basis of the high SAL partitioning in the micelle core, a stronger protective effect was expected compared to ionized SAL [17,18].

[DIMEB] wt %	*Core Radius*	*Shell Thickness*	*Volume fraction*	*Shell sld (x 10^6)/1/Å^2*

	Å	*Å*		
5	42	60	0.160	6.00
7	37	54	0.049	6.23
9	32	45	0.020	6.01
9*	35	57		6.17
13*	24	35		6.15
	Scale	*Rg/Å*		
11	0.29	26		

* data taken from [18]

Table 4. Fitting parameters obtained from SANS curves of SAL (1 wt%)-loaded F127 micelles (5 wt%) at pH=1 in D_2O at 37ºC with a CS-spheres model in the presence of varying amounts of DIMEB. 9*, 13*: fits to the curves at pH=7.

Interestingly, at 37ºC and 50 ºC, the data could be fitted with spherical micelles, rather than cylindrical ones, from the lowest concentration of DIMEB (5 wt%). At 37ºC, the size of the aggregates (Figure 6C, Table 5) decreases from 101 to 77 Å, as DIMEB concentration increases from 5 to 9 wt%; the volume fraction of the micelles also decreases concomitantly, from 0.160 in the absence of DIMEB up to 0.02, at 9 wt% DIMEB; at 11 wt% the micelles are fully broken up and the data can be fitted to Gaussian coils. Instead, at 50ºC (Figure 6D, Table 5), the micelles also shrink from 112 to 101 Å with 5 and 7 wt% DIMEB, and maintain a constant size (102 Å) at 9 wt% and at 11 wt% DIMEB. Therefore temperature makes the micelle more stable against DIMEB disruption, as had been observed at pH=7 [17,18].

At both temperatures, it is possible to observe an excess intensity at low *q*, more pronounced at 50ºC, possibly denoting the presence of larger structures [90,91].

In summary, the loaded micelles become more stable against DIMEB disruption as temperature increases, as observed for the free and SAL-loaded micelles at pH=7 (no data of free micelle at pH=1 is available). The effect of the temperature on the DIMEB disrupting ability has not been studied in depth, but it seems to be related the ability of the DIMEB to get in contact to the core [18]. Taking into account at pH=1 the water content increases with temperature this result suggests the water molecules inside the micelle package tighter as temperature increases making DIMEB diffusion, and therefore the breaking up, more difficult.

%DIMEB	*Radius Å*	*Thickness Å*	*Volume fraction*	*Shell sld (10^6)/ 1/Å^2*
5	48	64	0.225	6.0
7	41	60	0.166	6.1
9	41	61	0.134	6.1

11	------	------	------	------

Table 5. Fitting parameters obtained from SANS curves of SAL (1 wt%)-loaded F127 micelles (5 wt%) at pH=1 in D_2O at 50ºC with a CS-spheres model in the presence of varying amounts of DIMEB.

Deleted: .

The effect of pH can be assessed by comparing micellar size in the presence of DIMEB at pH=1 and 7. Ionized SAL-loaded micelles (pH=7), in the presence of 9 wt% DIMEB, present the same size (92 Å [18]) as the molecular SAL-loaded micelles (pH=1) with 7% DIMEB (91 Å, Table 4), and clearly higher than with 9% DIMEB (77 Å, Table 4) at pH=1. With 13 % DIMEB at pH=7, small micelles (59 Å) are still present whereas at pH=1 they are fully broken up with 11 wt% DIMEB.

For intestine-controlled release, SAL formulation should have a DIMEB concentration higher than 13% (DIEMB concentration which completely breaks up the loaded micelle at pH=7) [18]; but the present results show that at this DIMEB concentration, the micelles would be broken up in the stomach releasing the loaded SAL and therefore not avoiding the side effect of the drug which preclude oral administration of the drug.

In order to obtain further information about the disruptive effect of DIMEB, and assess whether the lower competition of SAL with F127 for DIMEB contributes to the non protective effect [18,90], the binding constant of molecular SAL (pH=1) to DIMEB, K_{DIMEB}, at 25 and 37ºC, was determined in H_2O and D_2O (SI5). Binding constants K_{DIMEB} = 483 g/g (25ºC) and K_{DIMEB} = 438 g/g (37ºC) were obtained at pH=1. No difference in the binding ability was found in D_2O at pH=1. The binding constants at pH=1 are of the same order as at pH=7, K_{DIMEB} = 440.9 g/g (25ºC) [17] and K_{DIMEB} = 423.3 g/g (37ºC) [18]. In contrast, using potentiometry, a much larger difference in the complexation ability between molecular SAL, K_{DIMEB} = 1570 M^{-1}, and ionized SAL, K_{DIMEB} = 140 M^{-1} with DIMEB had been reported [92], contrasting with our data. If we indeed assumed a larger DIMEB-SAL binding at pH=1, the free DIMEB available to interact with F127 micelles would be lower at pH=1 than pH=7, which would contribute to protect the micelles, not make it more suceptible to disruption as observed here.

Overall, we find that micelles at pH=1, with a high load of molecular SAL, are more susceptible to disruption by DIMEB than at pH=7 (where a very low amount of SAL partitions). Therefore, in a ternary formulation, the load would be released in the stomach. However, on the basis of partitioning, F127 micelles can efficiently solubilize SAL, retain it in the stomach and release it in the intestine, triggered by a change at physiological pH without DIMEB involvement. This effect has also been observed in P104 loaded with drugs with acid-basic properties [93], and it would be expected for SAL in P85 [27]. In comparison however, Pluronic F127 shows a higher solubilization ability (>19 molecules/micelle, estimated from solubility data) than P85 (8 molecules/micelle) [27]. In addition, the lower cmc of F127 (2.8×10^{-6}M) compared to P85 (6.5×10^{-5}M) reported [8] makes the micelle less susceptible to dilution effects in the body. In addition, the ability of F127 to form gels (at higher concentrations) make it a more attractive formulation for SAL (and other drugs with gastro intestinal side effects).

From a mechanistic point of view, previous time-resolved SANS and NMR studies have suggested that the interaction between the methyl groups of DIMEB and PPO may be responsible for the instantaneous break-up of the micelles [94], and that drugs loaded within the micelles (in addition to their ability to bind to DIMEB through inclusion complexes) may modulate the interactions between DIMEB and the PPO blocks [18], in particular by preventing interactions between DIMEB and PO units [16,18]. Sodium salicylate partitions very weakly inside the micelles (Table 1) and its location could not be determined by 2D NOESY NMR, whereas salicylic acid (in unionized form) is clearly located in the core [18], and in high quantities (as reflected by a high partition coefficient described in the present work). It is therefore all the more surprising that salicylic acid provides less protection against micellar disruption by DIMEB than salicylate anions.

All these results taken together suggest that the high hydration of the SAL-loaded micellar core, together with a higher separation between the polymer chains in the core to accommodate water, compared to pH=7 at a given temperature, may favor the diffusion of DIMEB through the micellar core and hence its interaction with PPO, which would therefore support the proposed mechanism DIMEB-triggered mechanism of disruption.

3.5. Cloud Point (CP) determination

The solubility of triblock co-polymers decreases with temperature, because water becomes a poorer solvent for PPO and PEO [95], ultimately leading to phase separation, or a cloud point, at high temperatures. Therefore, the cloud point is an easily measurable property of polymeric micelles sensitive to water content. For this reason, the cloud point of F127 (5wt %) in D_2O, free and loaded with SAL, was determined at pH=1 and pH=7 (Table 6).

	CP		**CP/ NaCl 2M/ D_2O**	
System/D_2O	**pH=7**	**pH=1**	**pH=7**	**pH=1**
F127	>98	>98	59	64
SAL 1%	>98	81	50	46-47
SAL1%/H_2O		87		

Table 6. Cloud point of F127 (5 wt%), free and with 1 wt% SAL at pH=1 and pH=7, in D_2O in the absence and presence of 2M NaCl. The cloud point for SAL-loaded micelles at pH=1 in H_2O is also included.

Free F127 micelles at pH=1 and pH=7, and SAL-loaded micelles at pH=7, all present a CP above 98ºC (the highest temperature measured). In contrast, in the presence of molecular SAL (pH=1), the CP drops to 81ºC (87 ºC in H_2O). The same effect was described for SAL on the CP of P85 micelles [27]. A decrease in CP is generally attributed to micellar dehydration [27,29,81] and an increase to micelle hydration [27,95], usually

in the region of the shell rather than the core [27], leading even to complete PEO dehydration [96].

In order to compare the CP of free and SAL-loaded F127 micelles at pH=1 and pH=7, the CP was shifted to lower temperatures by the addition of 2M NaCl. The CP of the free micelles at pH=7 (62ºC) is in agreement with the value previously reported under the same conditions [29]. As can be observed in Table 6, the CP of free F127 micelles at pH=1 is slightly higher than at pH=7, which is attributed to the salting-in effect of hydrogen ions in non-ionic surfactants [97,98]. This behavior is in good agreement with a higher micellar hydration at pH=1. However, despite similar values of shell hydration observed for free and loaded micelles at 50 ºC (Tables 2,3), and the higher water content of the core in the loaded micelles, the presence of SAL at pH=1 produces an effect opposite to predictions in decreasing the CP. The decrease of the CP produced by the addition of salts has been explained by the strong solvation of salts, which act "*as a pump"* to dehydrate the PEO [29], decreasing the solubility of the polymer and then its CP [29]. Therefore, given that the drug in its molecular form seems to bind strongly with the water molecules in the micelle, it is possible to speculate that it makes the polymer chains in the core less solvated than in its absence, despite the higher water content of the core in the loaded micelle. This behavior suggests the loaded aggregates need more water to be solubilized than the free ones, so when the micelle is not able to retain enough water the phase separation occurs, thus lowering the CP.

Surprisingly, the presence of SAL in ionized form also decreases the CP compared to free F127. This result is in good agreement to the decrease produced by ionized hydrochlorothiazide, CP=51 ºC (which has a very different structure than SAL), in the presence of 2M of NaCl [29]. However salicylate increased the CP of P85, in the absence of NaCl [27]. It is worthy to note that in these conditions the effect produced by molecular SAL and ionized SAL is nearly the same, unlike in the absence of salt. So, in these conditions the system becomes very complex and a more detailed study would required.

While the characterization of the behavior of the water pools inside the micelles is not an easy task, these results give support to the idea that water has a fundamental role in all the processes that sustain micellar behavior, including drug solubilisation and release, and interactions with a third compound, as DIMEB in this study.

4. Conclusion

F127 strongly increases the aqueous solubility of salicylic acid (SAL). SAL partitions significantly more in F127 micelles at pH=1 compared to pH=7, due to the absence of charge on the drug. The photophysical behavior of SAL reveals that the drug in the micelles forms intermolecular hydrogen bonds, possibly with F127, however further spectroscopy results suggest that it may instead be with water molecules. Quenching of SAL fluorescence inside the micelles is observed with increasing temperature, demonstrating that the vibration of the polymer chain forming the micellar core (where SAL is solubilized) increases with temperature. Nile red fluorescence shows that SAL-loaded micelles are more hydrated than the free micelles, with 30 and 17% of water in the core, respectively. SANS data analysis suggests that cylindrical micelles are formed at temperatures above 37ºC, whose core seems to be more hydrated than at lower

temperatures: (17 vs 23 % and 33 vs 35% at 37 ºC vs 50 ºC for free and SAL-loaded F127 micelles, respectively). The rearrangement of the water is suggested to be the main driving force for the sphere-to-cylinder shape transition. Despite the high amount of SAL molecules in the core, their presence does not afford protection to the micelles against disruption by DIMEB. In this case, the increased water content is likely to promote DIMEB diffusion, making interaction with the PO units in the core easier, which is one of the suggested mechanisms of micellar disruption. The presence of salicylic acid strongly decreases the CP of the loaded aggregate, which allows us to speculate that SAL indeed strongly binds the water molecules in the micellar core, decreasing PPO hydration.

From a practical point of view, F127 micelles are an efficient carrier of large amounts of drug; in addition, they can provide controlled intestinal release triggered by physiological changes in pH experienced by drugs after oral administration.

All the data taken together suggest that the water content is key to the re-arrangement of the polymer chains in the core of the aggregates, giving rise to a change in micellar morphology and also affecting the interaction of DIMEB with the micellar core, therefore facilitating the disruptive action of the cyclodextrins, and thus a controlled release mediated by this interaction. Overall, our results provide precious insights into the molecular interactions regulating drug loading and release in micellar nanocarriers and in more complex (ternary) systems, which provide a basis to rationalize formulation design.

Acknowledgements

This work is based upon experiments performed at the KWS-2 instrument operated by JCNS at the Heinz Maier-Leibnitz Zentrum (MLZ), Garching, Germany. This work benefited from the use of the SasView application, originally developed under NSF Award DMR- 0520547. SasView also contains code developed with funding from the EU Horizon 2020 programme under the SINE2020 project. Grant No 654000.

References

[1] A.M. Bodratti, P. Alexandridis, Formulation of poloxamers for drug delivery, J. Funct. Biomater. 9 (2018). https://doi.org/10.3390/jfb9010011.

[2] A.R. Fares, A.N. Elmeshad, M.A.A. Kassem, Enhancement of dissolution and oral bioavailability of lacidipine via pluronic P123 / F127 mixed polymeric micelles : formulation , optimization using central composite design and in vivo bioavailability study, 7544 (2018). https://doi.org/10.1080/10717544.2017.1419512.

[3] H. Shen, S. Liu, Enhancement of oral bioavailability of magnolol by encapsulation in mixed micelles containing pluronic F127 and L61, 70 (2018) 498–506. https://doi.org/10.1111/jphp.12887.

[4] X. Wu, W. Ge, T. Shao, W. Wu, J. Hou, L. Cui, J. Wang, Z. Zhang, Enhancing the oral bioavailability of biochanin A by encapsulation in mixed micelles containing Pluronic F127 and Plasdone S630, Int. J. Nanomedicine. (2017) 1475–1483. https://doi.org/http://dx.doi.org/10.2147/IJN.S125041.

[5] Z. Zhang, C. Cui, F. Wei, H. Lv, Improved solubility and oral bioavailability of apigenin via Soluplus / Pluronic F127 binary mixed micelles system, 9045 (2017).

https://doi.org/10.1080/03639045.2017.1313857.
[6] E. V Batrakova, A. V Kabanov, Pluronic block copolymers : Evolution of drug delivery concept from inert nanocarriers to biological response modi fi ers, J. Control. Release. 130 (2008) 98–106. https://doi.org/10.1016/j.jconrel.2008.04.013.
[7] M. Agafonov, T. Volkova, R. Kumeev, E. Chibunova, I. Terekhova, Impact of pluronic F127 on aqueous solubility and membrane permeability of antirheumatic compounds of different structure and polarity, J. Mol. Liq. 274 (2019) 770–777. https://doi.org/https://doi.org/10.1016/j.molliq.2018.11.060.
[8] A. V. Kabanov, E. V. Batrakova, V.Y. Alakhov, Pluronic block copolymers as novel polymer therapeutics for drug and gene delivery, J. Control. Release. 82 (2002) 189–212. https://doi.org/DOI: 10.1016/s0168-3659(02)00009-3.
[9] Y. Guan, J. Huang, L. Zuo, J. Xu, L. Si, J. Qiu, G. Li, Effect of Pluronic P123 and F127 Block Copolymer on P-glycoprotein Transport and CYP3A Metabolism, 34 (2011) 1719–1728. https://doi.org/10.1007/s12272-011-1016-0.
[10] Z. Wei, S. Yuan, J. Hao, X. Fang, Mechanism of inhibition of P-glycoprotein mediated efflux by Pluronic P123/F127 block copolymers: Relationship between copolymer concentration and inhibitory activity, Eur. J. Pharm. Biopharm. 83 (2013) 266–274. https://doi.org/10.1016/j.ejpb.2012.09.014.
[11] M.S.H. Akash, K. Rehman, S. Chen, Pluronic F127-based thermosensitive gels for delivery of therapeutic proteins and peptides, Polym. Rev. 54 (2014) 573–597. https://doi.org/10.1080/15583724.2014.927885.
[12] C.-C. Pai-Chie, F. Sylvan G, In vitro release of lidocaine from pluronic F-127 gels, Int. J. Pharm. 8 (1981) 89–99. https://doi.org/10.1016/0378-5173(81)90013-2.
[13] S. Demirci, E. Karaku, Z. Hal, A. Topçu, Boron and Poloxamer (F68 and F127) Containing Hydrogel Formulation for Burn Wound Healing, (2015) 169–180. https://doi.org/10.1007/s12011-015-0338-z.
[14] C. Di Donato, R. Iacovino, C. Isernia, G. Malgieri, A. Varela-garcia, A. Concheiro, C. Alvarez-lorenzo, Polypseudorotaxanes of Pluronic ® F127 with Combinations of α - and β -Cyclodextrins for Topical Formulation of Acyclovir, Nanomaterials. (2020). https://doi.org/10.3390/nano10040613.
[15] L.C. Gonçalves, A.B. Seabra, M.T. Pelegrino, D.R. De Araujo, J.S. Bernardes, Superparamagnetic iron oxide nanoparticles dispersed in Pluronic F127 hydrogel : potential uses in topical applications, RSC Adv. (2017) 14496–14503. https://doi.org/10.1039/C6RA28633J.
[16] M. Valero, C.A. Dreiss, Modulating Pluronics micellar rupture with cyclodextrins and drugs: Effect of pH and temperature, in: J. Phys. Conf. Ser., 2014. https://doi.org/10.1088/1742-6596/549/1/012010.
[17] M. Valero, C.A. Dreiss, Growth, shrinking, and breaking of pluronic micelles in the presence of drugs and/or β-cyclodextrin, a study by small-angle neutron scattering and fluorescence spectroscopy, Langmuir. 26 (2010). https://doi.org/10.1021/la100596q.
[18] M. Valero, F. Castiglione, A. Mele, M.A. Da Silva, I. Grillo, G. González-Gaitano, C.A. Dreiss, Competitive and Synergistic Interactions between Polymer Micelles, Drugs, and Cyclodextrins: The Importance of Drug Solubilization Locus, Langmuir. 32 (2016). https://doi.org/10.1021/acs.langmuir.6b03367.
[19] G. Wenz, B.H. Han, A. Müller, Cyclodextrin rotaxanes and polyrotaxanes, Chem. Rev. 106 (2006) 782–817. https://doi.org/10.1021/cr970027+.
[20] K. Kataoka, A. Harada, Y. Nagasaki, Block copolymer micelles for drug delivery:

927 design, characterization and biological significance, Adv. Drug Deliv. Rev. 47
928 (2001) 113–131. https://doi.org/10.1016/s0169-409x(00)00124-1.
929 [21] G. González-Gaitano, C. Müller, A. Radulescu, C.A. Dreiss, Modulating the self-
930 assembly of amphiphilic X-shaped block copolymers with cyclodextrins:
931 Structure and mechanisms, Langmuir. 31 (2015) 4096–4105.
932 https://doi.org/10.1021/acs.langmuir.5b00334.
933 [22] J. Puig-Rigall, I. Grillo, C.A. Dreiss, G. González-Gaitano, Structural and
934 Spectroscopic Characterization of TPGS Micelles: Disruptive Role of
935 Cyclodextrins and Kinetic Pathways, Langmuir. 33 (2017) 4737–4747.
936 https://doi.org/10.1021/acs.langmuir.7b00701.
937 [23] J. Puig-Rigall, R. Serra-Gómez, N. Guembe-Michel, I. Grillo, C.A. Dreiss, G.
938 González-Gaitano, Threading Different Rings on X-Shaped Block Copolymers:
939 Hybrid Pseudopolyrotaxanes of Cyclodextrins and Tetronics, Macromolecules.
940 (2020). https://doi.org/10.1021/acs.macromol.0c00409.
941 [24] M. Valero, I. Grillo, C.A. Dreiss, Rupture of pluronic micelles by Di-methylated
942 β-cyclodextrin is not due to polypseudorotaxane formation, J. Phys. Chem. B. 116
943 (2012). https://doi.org/10.1021/jp210439n.
944 [25] E.N. Loredana, A.P. Chiriac, M. Bercea, Effect of pH and temperature upon self-
945 assembling process between poly(aspartic acid) and Pluronic F127, Colloids
946 Surfaces B Biointerfaces. 119 (2014) 47–54.
947 https://doi.org/10.1016/j.colsurfb.2014.04.023.
948 [26] S. Alexander, W.M. De Vos, T.C. Castle, T. Cosgrove, S.W. Prescott, Growth
949 and shrinkage of pluronic micelles by uptake and release of flurbiprofen:
950 Variation of pH, Langmuir. 28 (2012) 6539–6545.
951 https://doi.org/10.1021/la204262w.
952 [27] P. Parekh, R. Ganguly, V.K. Aswal, P. Bahadur, Room temperature sphere-to-rod
953 growth of Pluronic® P85 micelles induced by salicylic acid, Soft Matter. 8 (2012)
954 5864–5872. https://doi.org/10.1039/c2sm25517k.
955 [28] M. Khimani, G. Verma, S. Kumar, P.A. Hassan, V.K. Aswal, P. Bahadur, pH
956 induced tuning of size, charge and viscoelastic behavior of aqueous micellar
957 solution of Pluronic®P104–anthranilic acid mixtures: A scattering, rheology and
958 NMR study, Colloids Surfaces A Physicochem. Eng. Asp. 470 (2015) 202–210.
959 https://doi.org/10.1016/j.colsurfa.2015.01.051.
960 [29] Y. Kadam, U. Yerramilli, A. Bahadur, P. Bahadur, Micelles from PEO-PPO-PEO
961 block copolymers as nanocontainers for solubilization of a poorly water soluble
962 drug hydrochlorothiazide, Colloids Surf. BBiointerface. 83 (2011) 49–57.
963 https://doi.org/10.1016/j.colsurfb.2010.10.041.
964 [30] M.R. Montinari, S. Minelli, R. De Caterina, The first 3500 years of aspirin history
965 from its roots – A concise summary, Vascul. Pharmacol. 113 (2019) 1–8.
966 https://doi.org/10.1016/j.vph.2018.10.008.
967 [31] C.C. d. Lima Silva, H.M. Shimo, R. de Felício, G.F. Mercaldi, S.A. Rocco, C.E.
968 Benedetti, Structure-function relationship of a citrus salicylate methylesterase and
969 role of salicylic acid in citrus canker resistance, Sci Rep 9. 3901 (2019) 3901.
970 https://doi.org/10.1038/s41598-019-40552-3.
971 [32] S.J. Bashir, F. Dreher, A.L. Chew, H. Zhai, C. Levin, R. Stern, H.I. Maibach,
972 Cutaneous bioassay of salicylic acid as a keratolytic, Int. J. Pharm. 92 (2005)
973 187–194. https://doi.org/doi:10.1016/j.ijpharm.2004.11.032.
974 [33] F. Food and Drug Administration, Title 21, volume 5, n.d.
975 [34] R. Labib, D. Bury, F. Boisleve, G. Eichenbaum, S. Girard, J. Naciff, M. Leal, J.
976 Wong, A kinetic-based safety assessment of consumer exposure to salicylic acid

977 from cosmetic products demonstrates no evidence of a health risk from
978 developmental toxicity, Regul. Toxicol. Pharmacol. 94 (2018) 245–251.
979 https://doi.org/10.1016/j.yrtph.2018.01.026.
980 [35] M. Almgren, F. Grieser, J.K. Thomas, Dynamic and static aspects of
981 solubilization of neutral arenes in ionic micellar solutions, J. Am. Chem. Soc. 101
982 (1997) 279−291. https://doi.org/10.1021/ja00496a001.
983 [36] G. Song, R. Guo, Y. Y.F, Fluorimetric deter mination of binding constants and
984 distribution coefficients of ethanol in the SDS micelles system, Yangzhou
985 Technol.Coll. (Nat.Sci.). 12 (1992) 42–47.
986 [37] A. Radulescu, N.K. Szekely, M.S. Appavou, V. Pipich, T. Kohnke, V. Ossovyi, S.
987 Staringer, G.J. Schneider, M. Amann, B. Zhang-Haagen, G. Brandl, M. Drochner,
988 R. Engels, R. Hanslik, G. Kemmerling, Studying soft-matter and biological
989 systems over a wide length-scale from nanometer and micrometer sizes at the
990 small-angle neutron diffractometer KWS-2, J. Vis. Exp. 2016 (2016) 1–23.
991 https://doi.org/10.3791/54639.
992 [38] M. Doucet, J.H. Cho, G. Alina, J. Bakker, W. Bouwman, P. Butler, K. Campbell,
993 M. Gonzales, R. Heenan, A. Jackson, P. Juhas, S. King, P. Kienzle, J. Krzywon,
994 A. Markvardsen, T. Nielsen, L. O'Driscoll, W. Potrzebowski, R. Ferraz Leal, T.
995 Richter, P. Rozycko, T. Snow, A. Washington, SasView version 4.2.2, (2019).
996 https://doi.org/10.5281/ZENODO.2652478.
997 [39] A. and G.F. Guinier, Small-Angle Scattering of X-Ray, John Wiley & Sons Inc,
998 new York, 1955.
999 [40] I. Livsey, Neutron Scattering from Concentric Cylinders, J. Chem. Soc., Faraday
1000 Trans. 2. 83 (1987) 1445–1452.
1001 [41] S.R. Kline, Reduction and analysis of SANS and USANS data using IGOR Pro, J.
1002 Appl. Crystallogr. 39 (2006) 895–900.
1003 https://doi.org/10.1107/S0021889806035059.
1004 [42] I. Grillo, I. Morfin, S. Prévost, Structural Characterization of Pluronic Micelles
1005 Swollen with Perfume Molecules, Langmuir. 34 (2018) 13395–13408.
1006 https://doi.org/10.1021/acs.langmuir.8b03050.
1007 [43] O. Glatter, O. Kratky, eds., Small Angle X-ray Scattering, Academic Press, 1982.
1008 [44] J.S. Higgins, H.C. Benoit, Polymers and Neutron Scattering, Oxford Science
1009 Publications, 1996.
1010 [45] S.M. King, Small Angle Neutron Scattering in Modern Techniques for Polymer
1011 Characterisation, Wiley, 1999.
1012 [46] G. González-Gaitano, M.A. Da Silva, A. Radulescu, C.A. Dreiss, Selective tuning
1013 of the self-assembly and gelation of a hydrophilic poloxamine by cyclodextrins,
1014 Langmuir. 31 (2015) 5645–5655. https://doi.org/10.1021/acs.langmuir.5b01081.
1015 [47] R. Serra-Gómez, C.A. Dreiss, J. González-Benito, G. González-Gaitano,
1016 Structure and rheology of poloxamine T1107 and its nanocomposite hydrogels
1017 with cyclodextrin-modified barium titanate nanoparticles, Langmuir. 32 (2016)
1018 6398–6408. https://doi.org/10.1021/acs.langmuir.6b01544.
1019 [48] J.H. Collett, R. Withington, Partition coefficients of salicylic acid between water
1020 and the micelles of some non-ionic surfactants, J. Pharm. Pharmacol. 24 (1972)
1021 211–214. https://doi.org/10.1111/j.2042-7158.1972.tb08966.x.
1022 [49] DrugBank, Salicylic acid, (2020).
1023 [50] Computed Properties by XLogP3 3.0 (PubChem release 2019.06.18), (n.d.).
1024 https://pubchem.ncbi.nlm.nih.gov/compound/156391 (accessed September 8,
1025 2020).
1026 [51] https://pubchem.ncbi.nlm.nih.gov/compound/Naproxen(accessed May 20, 2020).,

(n.d.).
[52] A. Choucair, A. Eisenberg, Interfacial Solubilization of Model Amphiphilic Molecules in Block Copolymer Micelles, J.Am.Chem.Soc. 125 (2003) 11993–12000. https://doi.org/10.1021/ja036667d.
[53] F. Gadelle, W.J. Koros, R.S. Schechter, Solubilization of Aromatic Solutes in Block Copolymers, Macromolecules. 28 (1995) 4883–4892. https://doi.org/10.1021/ma00118a014.
[54] H.C. Joshi, H.B. Tripathi, T.C. Pant, D.D. Pant, Hydrogen-bonding effect on the dual emission of salicylic acid, Chem. Phys. Lett. 173 (1990) 83–86. https://doi.org/10.1016/0009-2614(90)85307-X.
[55] H.C. Joshi, H. Mishra, H.B. Tripathi, Photophysics and photochemistry of salicylic acid revisited, J. Photochem. Photobiol. A Chem. 105 (1997) 15–20. https://doi.org/10.1016/S1010-6030(96)04565-0.
[56] D.D. Pant, H.C. Joshi, P.B. Bisht, H.B. Tripathi, Dual emission and double proton transfer in salicylic acid, Chem. Phys. 185 (1994) 137–144. https://doi.org/10.1016/0301-0104(94)00090-5.
[57] S. Maheshwari, A. Chowdhury, N. Sathyamurthy, H. Mishra, H.B. Tripathi, M. Panda, J. Chandrasekhar, Ground and Excited State Intramolecular Proton Transfer in Salicylic Acid: An Ab Initio Electronic Structure Investigation, J. Phys. Chem. A. 103 (1999) 6257–6262. https://doi.org/10.1021/jp9911999.
[58] H.C. Joshi, C. Gooijer, G. Van der Zwan, Water-induced quenching of salicylic anion fluorescence, J. Phys. Chem. A. 106 (2002) 11422–11430. https://doi.org/10.1021/jp020442s.
[59] R.N. de Souza, M.Z. Jora, L.G.T.A. Duarte, K.J. Clinckspoor, T.D.Z. Atvars, E. Sabadini, A new interpretation of the mechanism of wormlike micelle formation involving a cationic surfactant and salicylate, J. Colloid Interface Sci. 552 (2019) 794–800. https://doi.org/10.1016/j.jcis.2019.05.025.
[60] H. Mishra, V. Misra, M.S. Mehata, T.C. Pant, H.B. Tripathi, Fluorescence Studies of Salicylic Acid Doped Poly(vinyl alcohol) Film as a Water/Humidity Sensor, J. Phys. Chem. A. 108 (2004) 2346–2352. https://doi.org/10.1021/jp0309365.
[61] R.K. Rodrigues, M.A. Da Silva, E. Sabadini, Worm-like micelles of CTAB and sodium salicylate under turbulent flow, Langmuir. 24 (2008) 13875–13879. https://doi.org/10.1021/la802890x.
[62] J. V. Joshi, V.K. Aswal, P.S. Goyal, Effect of sodium salicylate on the structure of micelles of different hydrocarbon chain lengths, Phys. B Condens. Matter. 391 (2007) 65–71. https://doi.org/10.1016/j.physb.2006.08.050.
[63] P.B. Bisht, H. Petek, K. Yoshihara, U. Nagashima, Excited state enol-keto tautomerization in salicylic acid: A supersonic free jet study, J. Chem. Phys. 103 (1995) 5290–5307. https://doi.org/10.1063/1.470565.
[64] G.S. Denisov, N.S. Golubev, V.M. Schreiber, S.S. Shajakhmedov, A. V. Shurukhina, Effect of intermolecular hydrogen bonding and proton transfer on fluorescence of salicylic acid, J. Mol. Struct. 436–437 (1997) 153–160. https://doi.org/10.1016/S0022-2860(97)00136-1.
[65] S. Imadul Islam, A. Das, R.K. Mitra, Excited state proton transfer in reverse micelles: Effect of temperature and a possible interplay with solvation, J. Photochem. Photobiol. A Chem. 404 (2021). https://doi.org/10.1016/j.jphotochem.2020.112928.
[66] D.L. Sackett, J. Wolff, Nile red as a polarity-sensitive fluorescent probe of hydrophobic protein surfaces, Anal. Biochem. 167 (1987) 228–234. https://doi.org/10.1016/0003-2697(87)90157-6.

[67] D.L. Sackett, J.R. Knutson, J. Wolff, Hydrophobic surfaces of tubulin probed by time-resolved and steady-state fluorescence of Nile Red, J. Biol. Chem. 265 (1990) 14899–14906.
[68] A.M. Klinkner, P.J. Bugelski, C.R. Waites, C. Louden, T.K. Hart, W.D. Kerns, A novel technique for mapping the lipid composition of atherosclerotic fatty streaks by en face fluorescence microscopy, J. Histochem. Cytochem. 45 (1997) 743–753. https://doi.org/10.1177/002215549704500513.
[69] P. Greenspan, S.D. Fowler, Spectrofluorometric studies of the lipid probe, nile red, J. Lipid Res. 26 (1985) 781–789.
[70] T.M.R. Viseu, G. Hungerford, A.F. Coelho, M.I.C. Ferreira, Dye-host interactions for local effects recognition in homogeneous and nanostructured media, J. Phys. Chem. B. 107 (2003) 13300–13312. https://doi.org/10.1021/jp030284k.
[71] H. Tajalli, A.G. Gilani, M.S. Zakerhamidi, P. Tajalli, The photophysical properties of Nile red and Nile blue in ordered anisotropic media, Dye. Pigment. 78 (2008) 15–24. https://doi.org/10.1016/j.dyepig.2007.10.002.
[72] F. Palomba, D. Genovese, L. Petrizza, E. Rampazzo, N. Zaccheroni, L. Prodi, Mapping heterogeneous polarity in multicompartment nanoparticles, Sci. Rep. 8 (2018) 1–8. https://doi.org/10.1038/s41598-018-35257-y.
[73] C.P. Smyth, Dielectric Behavior and Structure, McGraw Hill, 1955.
[74] P. Walden, No Title, Z. Phys. 70 (1910) 569.
[75] I. Grillo, I. Morfin, J. Combet, Chain conformation: A key parameter driving clustering or dispersion in polyelectrolyte – Colloid systems, J. Colloid Interface Sci. 561 (2020) 426–438. https://doi.org/10.1016/j.jcis.2019.11.010.
[76] J.S. Pedersen, M.C. Gerstenberg, The structure of P85 Pluronic block copolymer micelles determined by small-angle neutron scattering, Colloids Surfaces A Physicochem. Eng. Asp. 213 (2003) 175–187. https://doi.org/10.1016/S0927-7757(02)00511-3.
[77] S. Manet, A. Lecchi, M. Impéror-Clerc, V. Zholobenko, D. Durand, C.L.P. Oliveira, J.S. Pedersen, I. Grillo, F. Meneau, C. Rochas, Structure of micelles of a nonionic block copolymer determined by SANS and SAXS, J. Phys. Chem. B. 115 (2011) 11318–11329. https://doi.org/10.1021/jp200212g.
[78] H.H. Kim, N.W. Song, T.S. Park, M. Yoon, Laser scanning confocal microscope (LSCM)-fluorescence spectral properties of Nile Red embedded in polystyrene film of different thickness, Chem. Phys. Lett. 432 (2006) 200–204. https://doi.org/10.1016/j.cplett.2006.10.049.
[79] T.H. Kim, Y.S. Han, J.D. Jang, B.S. Seong, SANS study on self-assembled structures of Pluronic F127 triblock copolymer induced by additives and temperature, J. Appl. Crystallogr. 47 (2014) 53–59. https://doi.org/10.1107/S1600576713030094.
[80] K. Dehvari, K.-S. Lin, S.S.-S. Wang, Small angle x-ray scattering characterization of multifunctional iron oxide-pluronic nanocarriers: Effect of temperature and drug encapsulation, Nanosci. Nanotechnol. Lett. 8 (2016) 667–670. https://doi.org/doi:10.1166/nnl.2016.2210.
[81] J. Dey, S. Kumar, S. Nath, R. Ganguly, V.K. Aswal, K. Ismail, Additive induced core and corona specific dehydration and ensuing growth and interaction of Pluronic F127 micelles, J. Colloid Interface Sci. 415 (2014) 95–102. https://doi.org/10.1016/j.jcis.2013.10.019.
[82] V. Shah, B. Bharatiya, V. Patel, M.K. Mishra, A.D. Shukla, D.O. Shah, Interaction of salicylic acid analogues with Pluronic® micelles: Investigations on micellar growth and morphological transition, J. Mol. Liq. 277 (2019) 563–570.

https://doi.org/10.1016/j.molliq.2018.12.142.
[83] K. Kaizu, P. Alexandridis, Glucose-induced sphere to ellipsoid transition of polyoxyethylene-polyoxypropylene block copolymer micelles in aqueous solutions, Colloids Surfaces A Physicochem. Eng. Asp. 480 (2015) 203–213. https://doi.org/10.1016/j.colsurfa.2014.10.061.
[84] Y. Kadam, R. Ganguly, M. Kumbhakar, V.K. Aswal, P.A. Hassan, P. Bahadur, Time Dependent Sphere-to-Rod Growth of the Pluronic Micelles: Investigating the Role of Core and Corona Solvation in Determining the Micellar Growth Rate, J.Phys.Chem. B. 113 (2009) 16296–16302. https://doi.org/10.1021/jp9036974.
[85] J. Puig-Rigall, M.J. Blanco-Prieto, A. Radulescu, C.A. Dreiss, G. González-Gaitano, Morphology, gelation and cytotoxicity evaluation of D-α-Tocopheryl polyethylene glycol succinate (TPGS) – Tetronic mixed micelles, J. Colloid Interface Sci. 582 (2021) 353–363. https://doi.org/10.1016/j.jcis.2020.08.004.
[86] R. Basak, R. Bandyopadhyay, Encapsulation of hydrophobic drugs in pluronic F127 micelles: Effects of drug hydrophobicity, solution temperature, and pH, Langmuir. 29 (2013) 4350–4356. https://doi.org/10.1021/la304836e.
[87] K.C. Shih, Z. Shen, Y. Li, M. Kröger, S.Y. Chang, Y. Liu, M.P. Nieh, H.M. Lai, What causes the anomalous aggregation in pluronic aqueous solutions?, Soft Matter. 14 (2018) 7653–7663. https://doi.org/10.1039/c8sm01096j.
[88] Y. Wang, S.A. Sukhishvili, Hydrogen-bonded polymer complexes and nanocages of weak polyacids templated by a Pluronic® block copolymer, Soft Matter. 12 (2016) 8744–8754. https://doi.org/10.1039/c6sm01869f.
[89] S. Alexander, T. Cosgrove, T.C. Castle, I. Grillo, S.W. Prescott, Effect of temperature, cosolvent, and added drug on pluronic-flurbiprofen micellization, J. Phys. Chem. B. 116 (2012) 11545–11551. https://doi.org/10.1021/jp303185m.
[90] C.A. Dreiss, E. Nwabunwanne, R. Liu, N.J. Brooks, Assembling and de-assembling micelles: Competitive interactions of cyclodextrins and drugs with Pluronics, Soft Matter. 5 (2009) 1888–1896. https://doi.org/10.1039/b812805g.
[91] C. Perry, P. Hébraud, V. Gernigon, C. Brochon, A. Lapp, P. Lindner, G. Schlatter, Pluronic and β-cyclodextrin in water: from swollen micelles to self-assembled crystalline platelets, Soft Matter. 7 (2011) 3502–3512. https://doi.org/10.1039/C0SM01092H.
[92] E. Junquera, L. Peña, E. Aicart, Binding of sodium salicylate by β-cyclodextrin or 2,6-di-o-methyl-β- cyclodextrin in aqueous solution, J. Pharm. Sci. 87 (1998) 86–90. https://doi.org/10.1021/js970117u.
[93] M. Khimani, G. Verma, S. Kumar, P.A. Hassan, V.K. Aswal, P. Bahadur, pH induced tuning of size, charge and viscoelastic behavior ofaqueous micellar solution of Pluronic®P104–anthranilic acidmixtures: A scattering, rheology and NMR study, Colloids Surfaces A Physicochem. Eng. Asp. 470 (2015) 202–210. https://doi.org/10.1016/j.colsurfa.2015.01.051.
[94] F. Castiglione, M. Valero, C.A. Dreiss, A. Mele, Selective interaction of 2,6-Di-O-methyl-β-cyclodextrin and pluronic F127 micelles leading to micellar rupture: A nuclear magnetic resonance study, J. Phys. Chem. B. 115 (2011). https://doi.org/10.1021/jp203753r.
[95] R.C. Da Silva, W.J. Loh, Effect of Additives on the Cloud Points of Aqueous Solutions of Ethylene Oxide–Propylene Oxide–Ethylene Oxide Block Copolymers, Colloid Interface Sci. 202 (1998) 385–390. https://doi.org/https://doi.org/10.1006/jcis.1998.5456.
[96] C.D. Grant, K.E. Steege, M.R. Bunagan, E.W. Castner Jr, Microviscosity in Multiple Regions of Complex Aqueous Solutions of Poly(ethylene oxide) oxide)-

poly(propylene oxide) oxide)-poly(ethylene oxide), J. Phys. Chem. B. 109 (2005) 22273–22284. https://doi.org/10.1021/jp053929k.
[97] H. Schott, E.A. Royce, Colloids and Surfaces, 19 (1986), Colloids Surf. 19 (1986) 399–418.
[98] A.M. AI-Ghamdi, H.A. Nasr-E1-Din, SURFACES, Colloids Surfaces A Physicochem. Eng. Asp. 125 (1997) 5–18.